

MATHEMATICAL MODELING OF BIRD GROUP BEHAVIOR

By

AYLIN AYDOGDU

A thesis submitted to the

Graduate School-Camden

Rutgers, The State University of New Jersey

In partial fulfillment of the requirements

For the degree of Master of Science

Graduate Program in Computational and Integrative Biology

Written under the direction of

Dr. Benedetto Piccoli and Dr. William Saidel

and approved by

---

Dr. Benedetto Piccoli

---

Dr. William Saidel

---

Simon Garnier

Camden, New Jersey

May, 2016

## THESIS ABSTRACT

Mathematical Modeling of Birds Group Behavior

By AYLIN AYDOGDU

Thesis Director:

Dr. BENEDETTO PICCOLI

In this paper we introduce two different models to study the group dynamic of birds on wire and taking off the ground. To begin with, the first model is agent-based and encompasses attraction-repulsion forces and topological interactions. The model is firstly analyzed and then simulated to study the main properties. Then, we compare the achieved results with data from pictures taken in New Jersey. Two different image elaboration protocols allowed establishing a good agreement with the model. Moreover, we showed potential handiness by analyzing group organization features and dynamics of groups with landing new birds. To further complete the analysis we also introduced a birth-death process to include the modeling of landing and departing birds. Secondly, the second model inspired by videos of birds taking flight was created with options for two different methods that are metric and topological interactions. Furthermore, the model returns a graph displaying the number of birds in the air vs. the time that is very similar to the observed data that was analyzes via ImageJ. Comparing the topological and metric interaction, the topological method is less regular and has a longer front length. Lastly, many trends were observed when comparing the front velocities under various constraints.

## Part I

# First Project-Birds On The Wire

### 1 Introduction

We all know that birds perch on wires between telephone poles. The goal of this work is to account for their observed distribution quantitatively: we do so by creating a model that predicts the relative spacings between individual birds and comparing the model with experimental observations of the spacings in nature. Group behavior in animals has greatly interested researchers and naturalists in the past, and has received special attention in the last decades as an example of self-organization in nature. In recent years a number of quantitative methods, both computational and mathematical, were developed not only by biologists, ethologists and zoologists, but also by mathematicians, physicists and engineers. The corresponding vast literature is well reviewed in a number of articles, see for instance [17, 24, 10]. In simple words, most studies aim at showing how self-organization may emerge from relatively simple interaction rules among individuals. The interest is usually on the resulting patterns generated by such interactions. There are quite a few common ingredients in most models, including the presence of social forces which produce attraction (for mating, food search or to avoid predation) and repulsion (to avoid collisions or excessive crowding) among group members. The collection of data for groups on the move is not an easy task, especially for birds in the wild, even if the seminal papers [2, 3] were able to extract massive data from the monitoring large starling flocks. At the modeling level, one of the main lessons from these investigations was the observation that interactions between birds were topological, i.e. interaction of birds is based on a given number

of closest neighbors and not on their absolute distance.

A special example of groups on the move is represented by birds roosting on a wire.

The specific features of this phenomenon, especially its one-dimensional nature, permit the development mathematical models that are amenable to relatively simple analytical and numerical investigations. For the same reasons, an effective validation based on targeted data collection is also possible by simple tools.

Notwithstanding these attractive features, to our knowledge this is the first study to deal with birds on wires with a systematic quantitative approach.

Our work has proceeded in three steps: modeling, analysis, and validation, which we describe below. The first step of our work is the development of the mathematical model. Our mathematical model is based on three main features: agent-based dynamics, attraction-repulsion forces, and “topological” interactions. While a formal description is given in Section 2, we informally describe it here, also in relation to the literature.

Firstly, our model is agent-based, in the sense that each agent is singularly considered: the dynamics is described an ordinary differential equation for every bird in the group. The birds are indistinguishable for the dynamics, so no bird plays a special role and in particular there are no leaders. Many models used similar assumptions, among others [5, 6, 15, 22, 26]. However, other research lines have been looking at the collective dynamics by statistical or continuum models [4].

Secondly, in our model birds interact by social forces of attractive and repulsive type. Note that in the literature, forces of attraction and repulsion are sometimes combined with alignment, i.e. the attitude of birds to adjust their own velocities to neighbors in the group, see for instance [9, 25]. However this ingredient is not necessary in our case because we choose to postulate a first order dynamics, thus distinguishing ourselves from models that mimic the laws of mechanics [8]. Our model is instead more similar to those proposed in [7, 21, 26].

Thirdly, we assume topological interactions. In contrast, most models in the literature assume metric interactions, that is, each animal in the group interacts with all individuals who are within a given distance from it [5, 6, 12, 18]. However, as mentioned above, there is evidence that starlings interact with a given number of neighbors, that is, topologically. More precisely, each bird will interact with a preassigned number  $d$  of closest mates independently of their distance (which may be much smaller or much bigger than a fixed metric radius). Such modeling idea actually has a long history: already Hamilton [14] considered attraction to the nearest neighbor, while Aoki [1] used two-to-four interactions. The latter type of interactions was also used in a few subsequent studies [15, 16, 20, 22, 26].

The second step is the analytical and numerical study of the model. In particular we proved useful mathematical properties, such as the existence of solutions for all times, the preservation of the order between the birds, the avoidance of collisions, and the preservation of the barycenter of the group. Then, we moved on to numerical investigations, which demonstrate other key properties of the model. All simulations convergence to an equilibrium configuration that has interesting properties: it shows larger inter-animal spacing close to the group borders and this increase of inter-animal distances is more pronounced when the number of neighbors  $d$  is larger. In fact, we also provide a formula for the total length of the group as function of model parameters. In particular, our simulations are able to reproduce expected structures for birds on wires, with particular focus on the inter-animal distances as function of the position in the group.

Our final step was to compare the predictive distributions with patterns of birds found in the wild. We collected images of starlings and pigeons on various locations in New Jersey (Camden county). Out of the collected pictures, we selected more than hundred images fitting our admissibility criteria in terms of image quality, position of the group, and presence of local factors affecting group positioning (such

as obstacles or poles). The first challenging task was the determination of groups in each picture. We used uniform criteria detailed in Section 3, such as minimum size of five birds, same species, static conditions and others. We measured all inter-animal distances of the various groups. The inter-animal distance can be defined in terms of the position of the bird's head or bird's barycenter, thus we used two different methods: the first based on ImageJ and the skeletonize function to measure distance between birds' heads; the second based on Matlab to measure distance among birds' barycenters. The results were comparable for the two different methods. The main results of the experimental study can be summarized as follows:

- 1) Groups with more than nine birds show the same structure of inter-animal distances as the model simulations;
- 2) The variation among inter-animal distances in pictures is significantly more varied w.r.t. those of simulations;
- 3) The length of the group and coefficients of second order fittings of group structures show a linear dependence on the size of the group (in accordance with the results from our model);
- 4) There is a significant asymmetry in group shapes, which suggests possible handedness of birds. To further investigate this issue, we analyze movies that reveal pretty consistent direction of movements of incoming birds to the wire. However, we feel that the variability of measurements of pictures and some environmental condition (such as wind) for movies do not allow to claim a definite conclusion about handedness. Finally, we statistically analyzed the correlation between model results and picture measurements and shows a reasonably good correlation.

To complete our investigation and model the situation detected in movies, we designed a variation of our mathematical model by adding a birth-death Poisson process representing birds landing or taking off. The model is necessarily stochastic, thus we limited our analysis to compute the expected number of birds as function of the arrival and departure rate and to show, by simulations, that the structure of the group of this second model appears to be quite close to the structure of the original

one.

The paper is organized as follows. In Section 2, we describe the proposed agent-based model and analyze it theoretically and numerically. In Section 3, we describe the data collection and analysis process. Moreover, we show comparison of results with the model ones. Finally in Section 4, we illustrate the model that includes the birth-death process.

## 2 An attraction-repulsion model for birds on wires

We consider  $N$  birds moving on a wire, represented by a one-dimensional state space. The vector of birds' positions depends on time, due to the interactions among them, and is represented by  $x : \mathbb{R}_{\geq 0} \rightarrow \mathbb{R}^N$ . We assume that each component  $x_i(t)$ , representing the position of bird  $i \in \{1, \dots, N\}$ , satisfies the ODE

$$\dot{x}_i = \sum_{j \in \mathcal{N}(i)} \left( |x_j - x_i|^{m_a-1} - \xi^{m_a-m_r} |x_j - x_i|^{m_r-1} \right) (x_j - x_i) \quad \forall i \in \{1, \dots, N\}, \quad (1)$$

or equivalently

$$\begin{aligned} \dot{x}_i &= f_i(x) \quad \forall i \in \{1, \dots, N\} \\ f_i(x) &= \sum_{j \in \mathcal{N}(i)} |x_j - x_i|^{m_a} \frac{(x_j - x_i)}{|x_j - x_i|} - \xi^{m_a-m_r} \sum_{j \in \mathcal{N}(i)} |x_j - x_i|^{m_r} \frac{(x_j - x_i)}{|x_j - x_i|} \end{aligned} \quad (2)$$

where

- $\mathcal{N}(i)$  is the interaction neighborhood of bird  $i$ , that is, the set of birds that  $i$  is influenced by;
- $m_a \geq 0, m_r < 0$  are exponents that determine the attraction and repulsion forces, respectively (the two terms in (2));
- $\xi > 0$  is a desired distance between two birds, which compares the relative strengths of repulsion and attraction.

Observe that the dynamics (1) is invariant for translations, that is, it only depends on relative distances between pairs of birds and not on their absolute positions in a global reference frame.

In order to define the topological neighborhood in a concise way, we first assume that the birds are sorted so that  $x_i < x_j$  if  $i < j$  (we shall see later that this choice entails no loss of generality). Then, given  $d \in \mathbb{N}$ , we define

$$\mathcal{N}(i) = \{k \in \{1, \dots, N\} \mid |i - k| \leq d\}, \quad (3)$$

meaning that each animal interacts with  $d$  group mates on its left and  $d$  group mates on its right. Note that (3) implies that interactions are *symmetric*: if  $j \in \mathcal{N}(i)$ , then  $i \in \mathcal{N}(j)$ . This fact in turn implies that  $\frac{d}{dt} \left( \sum_{i=1}^N x_i \right) = 0$ , that is, the barycenter of the group is kept constant.

From a mathematical perspective, also note that the right-hand-side of (1) is not defined when  $x \in \mathcal{D}$ , with

$$\mathcal{D} = \{x \in \mathbb{R}^N \mid x_h = x_k \text{ for some } h \neq k\}.$$

We collect some basic but important properties of (1) in next Proposition.

**Proposition 2.1** (Fundamental properties of solutions). *Let  $x(t)$  satisfy (1) with neighborhoods (3) and  $x(0) = \bar{x} \in (\mathbb{R}^N \setminus \mathcal{D})$ , with  $\bar{x}_i > \bar{x}_j$  when  $i > j$ . Then,*

i) *a solution  $x(t)$  exists for all  $t > 0$ ;*

ii)  *$x_i(t) > x_j(t)$  for all  $t > 0$ ;*

iii) *defining  $x_{\text{ave}}(t) = \frac{1}{N} \sum_{k=1}^N x_k(t)$ , then  $x_{\text{ave}}(t) = x_{\text{ave}}(0)$ , for all  $t > 0$ .*

We stress that this result guarantees that the birds do not collide and do not change their order on the wire during the dynamics. We postpone the technical proof of Proposition 2.1 to the Appendix.

The long-time behavior of the solutions to (1) has been investigated through simulations, which support the following claim. Recall that  $x^* \in \mathbb{R}^N$  is said to be an equilibrium for (1), if  $f(x^*) = 0$ .

**Claim 1** (Convergence). *The solutions to (1) with neighborhood (3) converge to an equilibrium.*

Figure 1 shows an example of this observed convergence.

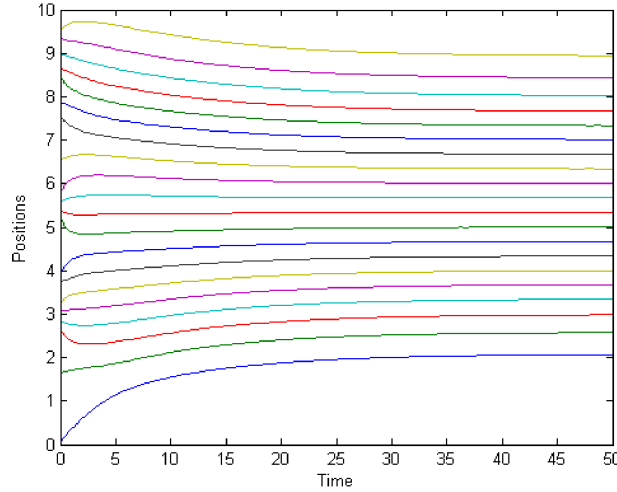


Figure 1: Positions of each individual bird as function of time, from random initial conditions for a group of  $N = 20$  birds with  $\xi = 1$ ,  $m_a = 0$ ,  $m_r = -2$ .

Furthermore, some properties of the equilibria can be studied analytically, as stated in the following simple result.

**Proposition 2.2** (Properties of equilibria). *Let  $x^* \in \mathbb{R}^N$  be such that  $f(x^*) = 0$ .*

*Then,*

- i)  $f(x^* + c\mathbf{1}) = 0$  for every  $c \in \mathbb{R}$ ;
- ii) for every  $i \in \{1, \dots, N\}$ , the normalized spacing  $\frac{x_{i+1}^* - x_i^*}{x_N^* - x_1^*}$  does not depend on  $\xi$ .

*Proof.* Notice that i) is immediate, as  $f(x)$  only depends on differences among

components of  $x$ . In order to prove ii), since

$$\begin{aligned} 0 &= \sum_{j \in \mathcal{N}_i} [(x_j - x_i)^{m_a} - \xi^{m_a - m_r} (x_j - x_i)^{m_r}] \\ &= L^{-m_a} \sum_{j \in \mathcal{N}_i} [(x_j - x_i)^{m_a} - \left(\frac{\xi}{L} L\right)^{m_a - m_r} (x_j - x_i)^{m_r}] \\ &= \sum_{j \in \mathcal{N}_i} \left[ \left(\frac{x_j - x_i}{L}\right)^{m_a} - \left(\frac{\xi}{L}\right)^{m_a - m_r} \left(\frac{x_j - x_i}{L}\right)^{m_r} \right], \end{aligned}$$

we can argue that for any  $m_a, m_r$ , if  $x$  is an equilibrium for system (1), then  $x/L$  is an equilibrium for the system with  $\xi$  replaced by  $\xi' = \frac{\xi}{L}$ , and this fact is equivalent to ii).  $\square$

This result has told us that the parameter  $\xi$  only plays a role in determining the total length of the group and does not influence how the birds distribute within the group. The intra-group distribution of the birds, instead, can be explored by simulations.

Our findings are summarized in the following statement and in the related discussion below.

**Claim 2** (Group center is denser). *If  $d = 1$ , then the equilibrium configuration is evenly spaced. If instead  $d > 1$ , then the animals are more widely spaced at the borders of the group. The increase in inter-animal distance becomes more pronounced as  $d$  grows.*

In order to support this claim, in Figure 2 we represent the equilibria reached at the end of simulations for various values of  $d$ . More precisely, we plot the (normalized) inter-animal distance as function of the bird position. From Figure 2 we see that the inter-animal distances are constant for  $d = 1$ , while they are larger close to the boundary of the group for  $d \geq 2$ . For  $d = 2$  we notice that the inter-animal distances are not monotonically increasing as we approach the border of the group:

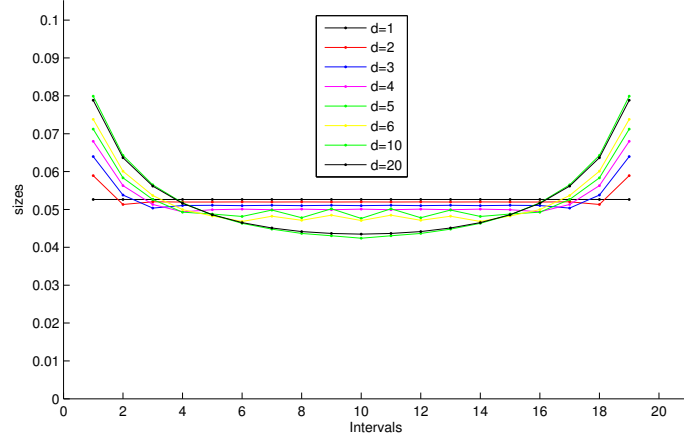


Figure 2: Distribution of normalized inter-animal distances at the equilibrium of (1);  $N = 20$ ,  $\xi = 1$ ,  $m_a = 0$ ,  $m_r = -2$ .

however, for larger  $d$  the monotonicity appear to be guaranteed.

We can also confirm that the increase in inter-animal distances, as we approach the borders of the group, is more pronounced as  $d$  increases. More precisely, for larger  $d$  (i.e. when there is more interaction), the intervals between birds at the extremities of the group are larger than the intervals between birds in the center. In other words, the more the birds interact with each other the more the sizes of the intervals vary.

**Claim 3** (Group length). *The total length  $L$  of the equilibrium configuration is proportional to  $\xi$  and to  $N - 1$ , and approximately  $L \approx \frac{\xi(N-1)}{\sqrt{d}}$ .*

In our example case,  $\xi = 1$  and  $N = 20$ , thus the length of the group is claimed to be proportional to  $\frac{19}{\sqrt{d}}$ . The comparison between this prediction and the group length obtained by simulations is reported in Figure 3, showing a pretty good agreement.

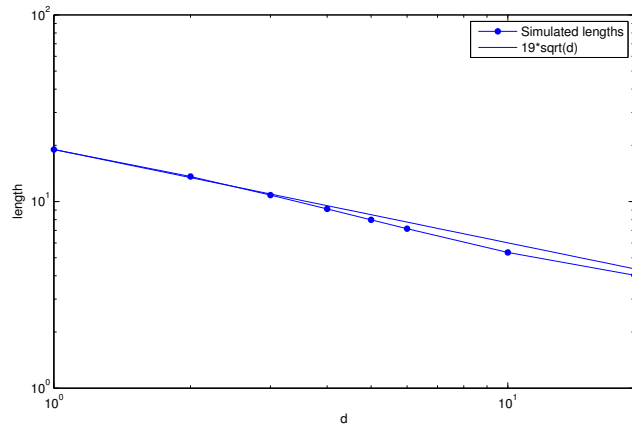


Figure 3: Total group length, as a function of  $d$ , for  $N = 20$ ,  $\xi = 1$ ,  $m_a = 0$ ,  $m_r = -2$ .

## 2.1 Asymmetric interactions and modeling of handedness

Motivated by our experimental results below, we are interested in verifying whether the observed birds exhibit a preference for interactions to their right or to their left—we refer to this feature as *handedness*. To this goal, we propose a variation of the model where each bird interacts with a different number of neighbors on its left ( $d_l$ ) and its right ( $d_r$ ), hereafter called the asymmetric case. More formally, in the asymmetric case the neighborhood definition becomes

$$\mathcal{N}(i) = \{k \in \{1, \dots, N\} \mid i - d_l \leq k \leq i + d_r\} \quad (4)$$

We now focus on the asymmetric case and compare it with the symmetric one. Moreover, we study the asymmetric case for different values for  $d_l$  and  $d_r$  and illustrate some results for the specific case in which the ratio  $d_l/d_r$  is kept constant: this quantity appears to determine the final configuration of the group. We have seen that the symmetric case satisfies the first claim and the velocities of the birds converge to zero and an equilibrium position is reached with constant inter-animal distances, see Figure 1. Instead, the asymmetric case does not satisfy the Claim 1 in a strict sense because, although the birds do reach stable inter-animal distances, they continue to drift as a whole, see Figure 4. Clearly, this unbounded motion can not be achieved in reality due to physical constraints of the wires. However, the asymmetric case satisfies Claim 2 as shown in Figure 5, where a concave up configuration is reached in inter-animal distances for the final configuration of the group. The concavity increases with increasing values of  $d$ .

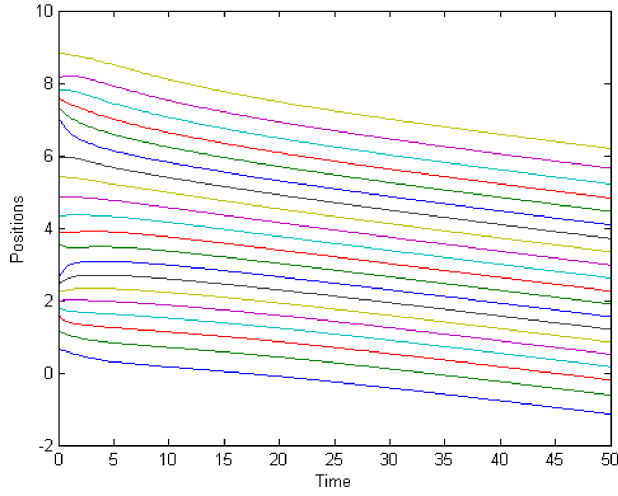


Figure 4: Positions of each individual bird as function of time in the asymmetric case.

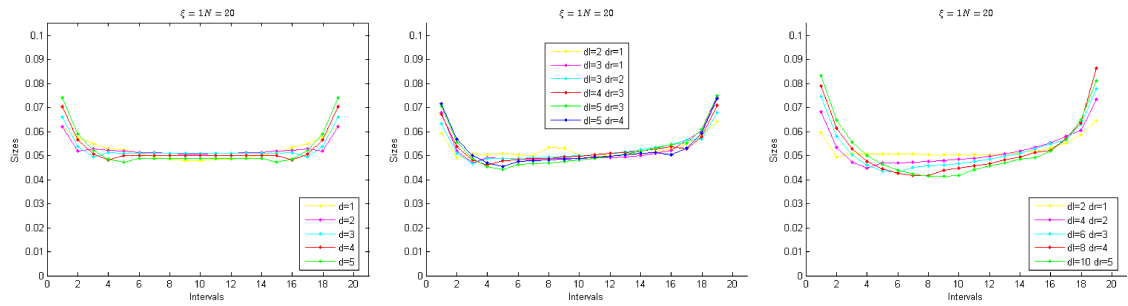


Figure 5: Final inter-animal spacing of starlings. Comparison of (left) symmetric case; (center) asymmetric case; (right) asymmetric case with constant ratio  $d_l/d_r = 2$ .

### 3 Model validation from experimental data

In order to validate the ODE model, fieldwork activity has been performed at locations in Camden County, South Jersey, with the goal of collecting images of birds on wires. By this activity, a set of 114 pictures of pigeons and starlings was collected, of which 108 imaged starling groups and 6 imaged pigeon groups. A single picture, however, can include several groups located on different wires: an example is in Figure 6. The main criteria adopted to identify different groups are the following:

- a group includes at least five birds;
- a group ends in case of pole, of course in case of lack of adjacent bird or in case the neighboring straight bird is too far off;
- all members of each group show the same side to the photographer;
- all members belong to the same species;
- all members are static (e.g. a bird has not taken off or landed on the wire in the immediate past);
- groups on crossing wires are not included, in order to avoid interactions not included in the model.



Figure 6: Left: Pigeons photo. Right: Starlings photo.

### 3.1 Methodology

To analyze and measure distance in photographs, we used ImageJ(version 1.47t) and two different methods.

**Method 1.** With this program, we were able to scale our pictures using a landmark directly measured in each photograph to produce a ratio of pixels to centimeter. ImageJ allowed us to crop the bird groups in the pictures, convert the images to binary to isolate the birds against a background of the sky, and skeletonize the image. The skeletonize function in ImageJ uses the black pixel clusters of a binary image and collapses them to a centerline 'skeleton' based on the center of mass of the cluster. Then, we were able to measure from the 'head', or top, of each skeleton to the next to gather our  $i$ -th spacing measurements and group length L measurements. (See Figure 7)

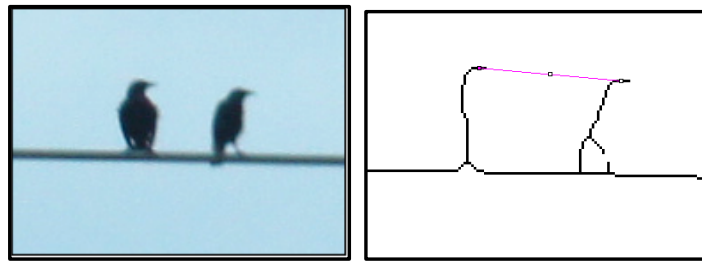


Figure 7: The crop of a bird group and its binary, skeletonized counterpart with measurement tool (magenta).

**Method 2.** We removed extraneous objects that have a size comparable to that of the birds and readjusted the contrast and brightness. We further processed our images using an algorithm in Matlab that performs the following:

1. Converts the image to black and white (see Figure 8).
2. Removes the wires on the pictures by removing clusters of pixels that have height that is relatively small compared to those of the birds.
3. Determines the centroid of each bird in terms of pixels.

4. Computes the distances between the centroids from left to right.

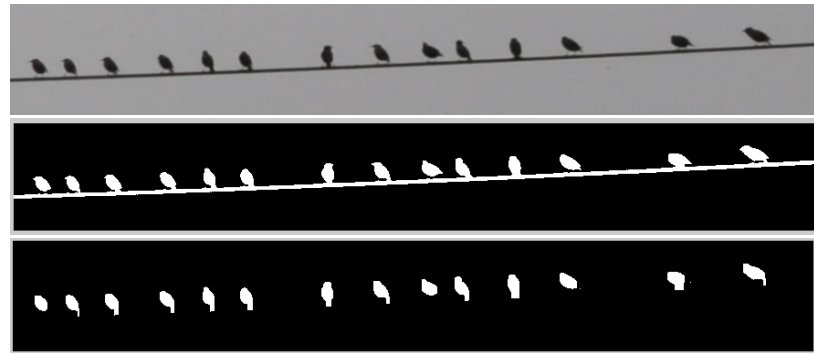


Figure 8: Processing images of bird groups with Matlab.

### 3.2 Analysis of images

We selected images and identified groups of birds adhering to the following criteria:

1. There had to be a minimum of 12 birds.
2. A group ends when the distances between two birds on the periphery exceed twice the average of the rest of the birds in the group.
3. The lens of the camera is perpendicular to the wire imaged in a photograph.

In Figure 9, the distance between adjacent pairs of birds is represented. A second-order regression curve shows a trend quite similar for both species ( $d = 20$  or  $d = 10$ ). These results conclusively demonstrate that the distance between pairs of birds is smaller in the middle of a group than near the borders of the group.

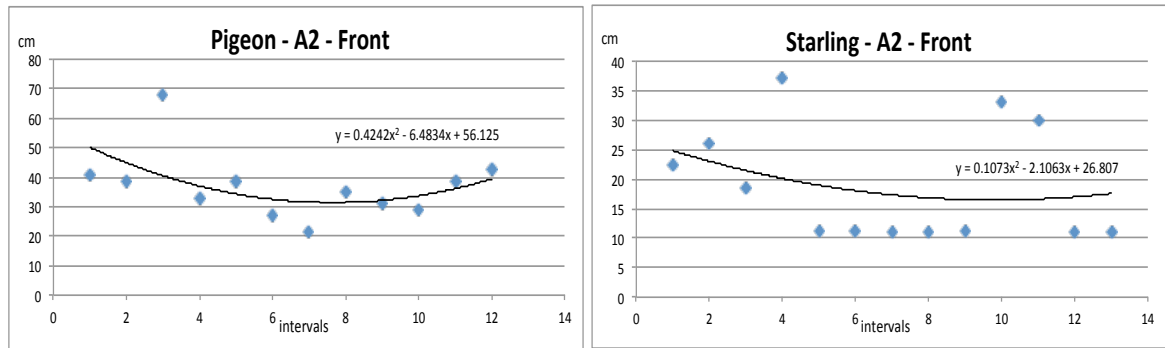
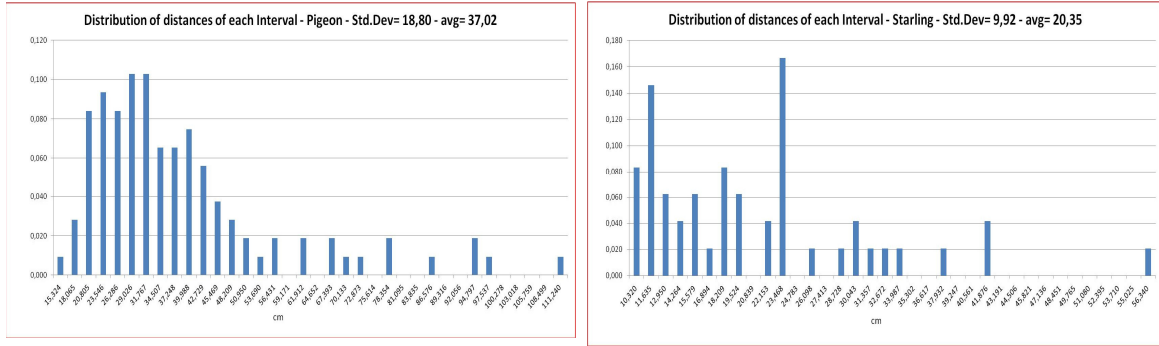


Figure 9: Left: Inter-pigeons distances. Right: Inter-starlings distances.

The distribution of distances between subsequent pairs is reported in Figure 10 for both pigeons and starlings. Small distances in the distribution of pigeons are more frequent and this is consistent with remarks describing Figure 9 that pairs of birds in the middle of a group closer than pairs at the borders.

Figure 11 on the left reports group lengths as a function of number of group couples (including all species, both starlings and pigeons). The regression line shows the global group length increases with number of birds but less quickly (a double couple number implies an increased length, but less than a double increase).



### 3.3 Correlation between simulations and images

To validate our model, we computed Pearson's correlation coefficients between the images and simulated symmetric case, and between the images and the simulated asymmetric non-proportional case. To attain statistical significance, only groups with a minimum of 3 corresponding images with the same number of birds were used. The model correlated reasonably well with measurements taken from the images across the ranges of  $\xi$  and  $d$  considered (Figures 12-13-14).

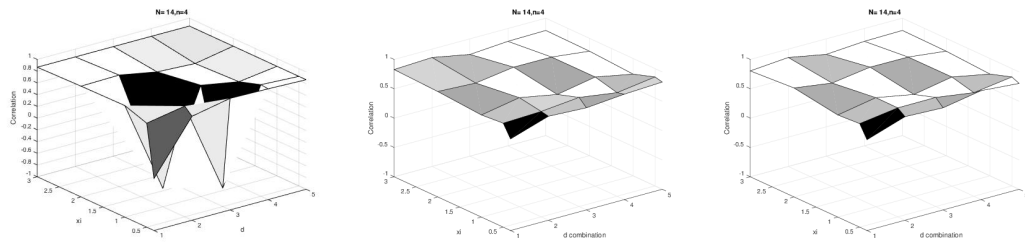


Figure 12: Pearson's correlation coefficients between the images with 14 birds and the simulations for the (left) symmetric case; (center) asymmetric and non-proportional increase case; and (right) asymmetric with fixed ratio  $d_l/d_r$ . The  $(d_l d_r)$  combinations in (center) and (right) are (2 1), (3 1), (3 2), (4 3), (5 3), (5 4) and (2 1), (4 2), (6 3), (8 4), (10 5), respectively.

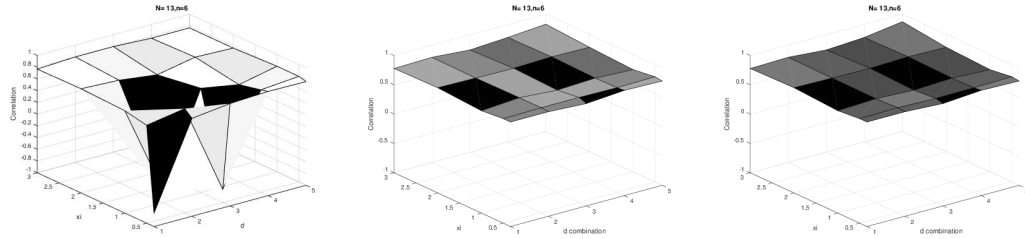


Figure 13: Pearson's correlation coefficients between the images with 13 birds and the simulations: (left) symmetric case; (center) asymmetric case; (right) asymmetric case with fixed ratio  $d_l/d_r$ .

We further evaluated the performances of symmetric and asymmetric and non-proportional increase cases by comparing the correlation coefficients between them using paired  $t$ -tests (Figure 15). Using a significance value of 0.05, we found that the number of the  $p$ -values greater than 0.05 ( $n = 99$ ) is significantly greater

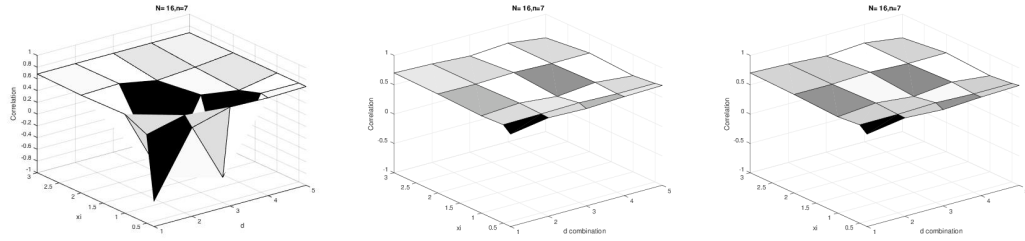


Figure 14: Pearson’s correlation coefficients between the images with 16 birds and the simulations: (left) symmetric case; (center) asymmetric case; (right) asymmetric case with fixed ration  $d_l/d_r$ .

than those less than 0.05 ( $n = 26$ ). This suggests that as far as this particular case goes, neither the symmetric nor the asymmetric and non-proportional increase case performed better than the other.

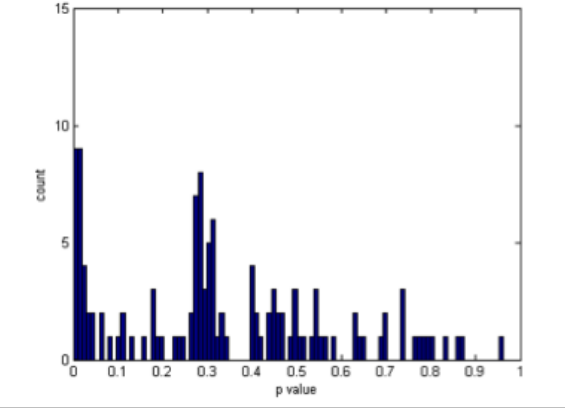


Figure 15: Distribution of  $p$ -values computed by varying  $d$  of the symmetric case and comparing it with all combinations of  $d$  for the asymmetric and non-proportional increase case. Note that the set of combinations of  $d$  (2 1), (3 1), (3 2), (4 3), (5 3) is used for the  $t$ -test.

### 3.4 Fitting quadratic curves

We now move to further analyse the fitting of second-order regression curves (parabolas), say  $a x^2 + b x + c$ , as in Figure 9. The analysis of coefficients  $a$  and  $b$ , fitting the distance between subsequent pairs of birds, sheds some light on birds behaviors. The behavior of coefficient  $a$  as function of number of birds in the group (all species) is illustrated in Figure 11 on the right. Since  $a$  measures the curvature of the parabola, the first order regression line shows as the curvature decreases with increasing number of birds. Notice that the shape of the distribution of distances, obtained by the model of Section 2, strongly depends on the parameter  $d$ , which represents the number of influential birds on each side of a focal individual. Here  $a$  and  $L$  are considered as functions of the number of all birds in the group. Both,  $a = g(\#intervals)$  and  $L = f(\#intervals)$  are invariant with respect to the side the birds show to the photographer (back or front, now shown graph).

We then investigated the dependence of the parameter  $-b/2a$  on the orientation of the group. More precisely, we postulate that, if birds show a preference for one direction (left or right), also called handedness, then the position of the vertex of the parabola (the parameter  $-b/2a$ ) should show consistent differences for groups facing the photographer or facing the opposite side. Since in our pictures birds always face the photographer, we measured the value  $-b/2a$  for all pictures organizing the inter-animal distances from left to right and from right to left. The results are summarized in Figure 16 for pigeons and Figure 17 for starlings. We notice that handedness may be present but data are not sufficient for a definite claim.

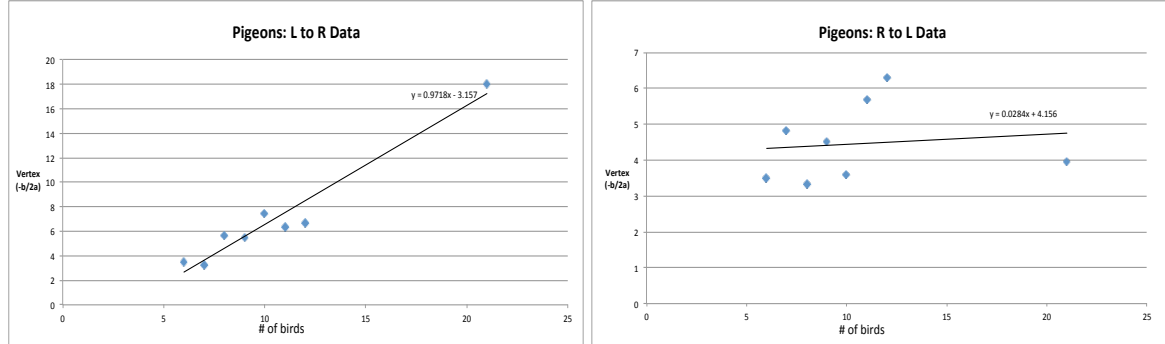


Figure 16: Pigeons:  $-b/(2a)$  as function of the intervals number.

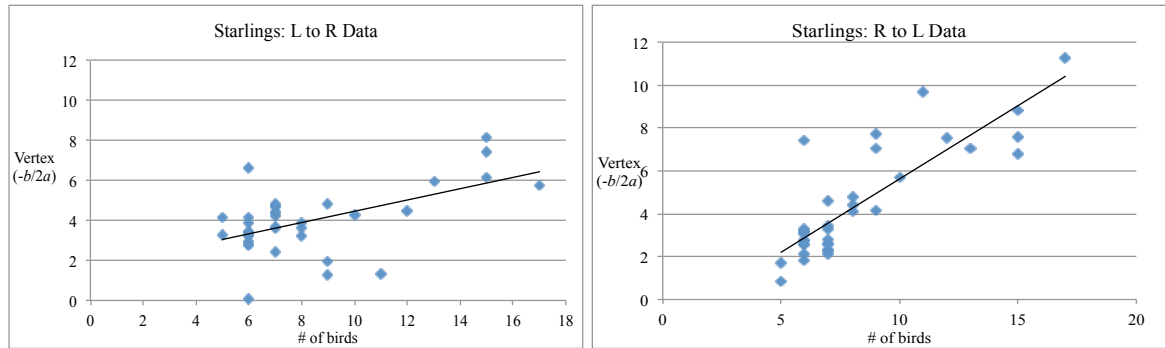


Figure 17: Starlings:  $-b/(2a)$  as function of the intervals number.

### 3.5 Analysis of movies and handedness

To further investigate our model validation and potential birds handedness, we considered movies of groups with new birds joining flying to the wire. If the birds lacked handedness, we assume the birds would shift in either direction without preference. If they possessed handedness, one direction would be preferred. All the movies taped starling groups.

We analyzed few movies of groups with a single new bird joining the group at a given position (not on the boundary of the group). A typical result is shown in Figure 18 where we represent the time intervals in which each bird moved. There is

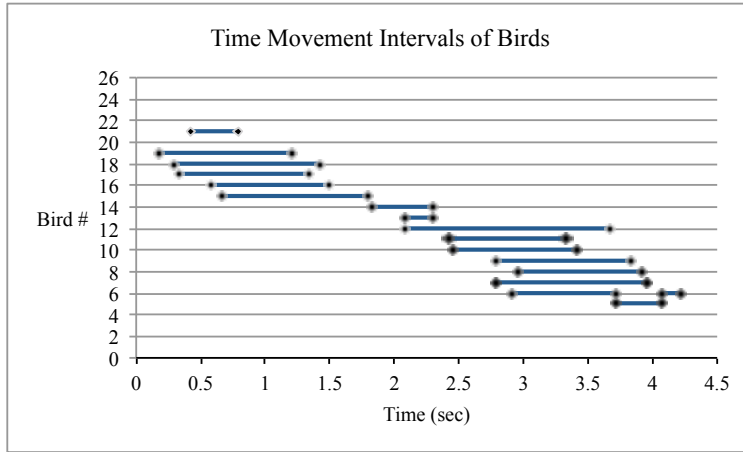


Figure 18: Starlings: Movement showing intervals in which each bird moved during movie, caused by bird number 20’s arrival into group.

a reasonable consistence of the time propagation of the signal of the new arrived bird, which is compatible with the model proposed in Section 2 with a limited number of interacting bird (i.e. finite  $d$ ). Moreover, we notice that the number of moving birds at each time varies between 2 and 5, thus suggesting that the range of  $d$  should indeed be between these values. Such results were consistent over all analyzed movies.

For handedness, we considered the direction of readjustments of birds already sitting on the wire. More precisely, in all movies a new arriving bird generated no

readjustment of the sitting birds or readjustment only towards one direction (w.r.t. to the arriving bird). The results are reported in Figure 19. We notice that the readjustments were always to the right or not present. Even if the data were

Direction of Movement of Groups			
	Left	Right	No Movement
Number of Groups	2	24	7

Figure 19: Starlings: directions of readjustments.

completely consistent with handedness, some caution should be taken because of additional potential factors, such as the direction of the wind and the direction of the incoming bird. Therefore, we can not conclude for birds handedness without further investigations.

## 4 A model with arrivals and departures of birds

As discussed in Section 3.5, in many cases the dynamics of birds on wires is affected by arriving and leaving birds. Therefore, we further elaborated the model of Section 2 by adding a stochastic description of the arrivals/departures of the birds. The rest of this section illustrates the obtained model and provides a preliminary analysis that is supported by simulations.

Let at time  $t \geq 0$  the animals be indexed in the finite, possibly empty, set  $\mathcal{I}(t) \subset \mathbb{Z}_{\geq 0}$ . We denote the cardinality of  $\mathcal{I}(t)$  by  $N(t)$ . At every time  $t \geq 0$ , we associate a position  $x_i(t) \in \mathbb{R}$  to every  $i \in \mathcal{I}(t)$ . Let there be an arrival Poisson process  $\{A(t)\}_{t \geq 0}$  of intensity  $\lambda > 0$  and, for each  $i \in \mathcal{I}(t)$ , a departure Poisson process  $\{D_i(t)\}_{t \geq 0}$  of intensity  $\mu_i > 0$ : we assume that all  $\mu_i$  are equal and denote them by  $\mu$ . Based on these processes, we construct the arrival-departure process as follows. If  $t_0$  is a jump time of the arrival process, then a bird is added to the group at time  $t_0$ , that is  $\mathcal{I}(t_0) = \mathcal{I}(t_0^-) \cup \{j\}$  with  $j \in \mathbb{Z}_{\geq 0} \setminus \mathcal{I}(t_0^-)$ ; clearly,  $N(t_0) = N(t_0^-) + 1$ . The position of the new animal is  $x_j(t_0) = z$ , where  $z$  is the realization of a real-valued random variable  $Z$ , whose law should depend on  $x(t)$ .

We choose

$$Z \sim \begin{cases} \mathcal{N}\left(\frac{\sum_k x_k(t_0^-)}{N(t_0^-)}, \frac{\sum_{h,k} (x_h(t_0^-) - x_k(t_0^-))^2}{N(t_0^-)-1}\right) & \text{if } N(t_0^-) \geq 2 \\ \mathcal{N}(x_1(t_0^-), \xi) & \text{if } N(t_0^-) = 1 \\ \mathcal{N}(0, \xi) & \text{if } N(t_0^-) = 0 \end{cases} \quad (5)$$

where  $\mathcal{N}(a, b)$  denotes a Gaussian distribution with mean  $a$  and variance  $b$ . This choice ensures that the arriving birds join the group by approximately landing in the area that is already occupied by the group. Correspondingly, if  $t$  is the first jump time of the  $i$ -th departure process, then  $\mathcal{I}(t^+) = \mathcal{I}(t) \setminus \{i\}$ , and in particular  $N(t^+) = N(t) - 1$ . Due to our assumptions, it is immediate to recognize that the number of animals  $N(t)$  follows a birth-death process with birth rate  $\alpha$  and death

rate  $N(t)\mu$ : consequently, standard deductions [11, Sect. 6.11] yield that the process asymptotically converges to its unique stationary distribution, which is a Poisson distribution with parameter  $\frac{\lambda}{\mu}$ : in particular,  $\lim_{t \rightarrow \infty} \mathbb{E}[N(t)] = \frac{\lambda}{\mu}$ .

Between the jumps of the processes, we assume that the system evolves in  $\mathbb{R}^{\mathcal{I}(t)}$  according to (1). Clearly, if the rates  $\lambda$  and  $\mu$  are very small, the process will behave approximately like (1). In fact, simulations show that in spite of the disturbances due to arrival and departures, the process is able to maintain a well-spaced configuration, even when the rates are relatively large. Two sample simulations are provided in Figure 20, which are qualitatively consistent with the behaviors observed in the movies.

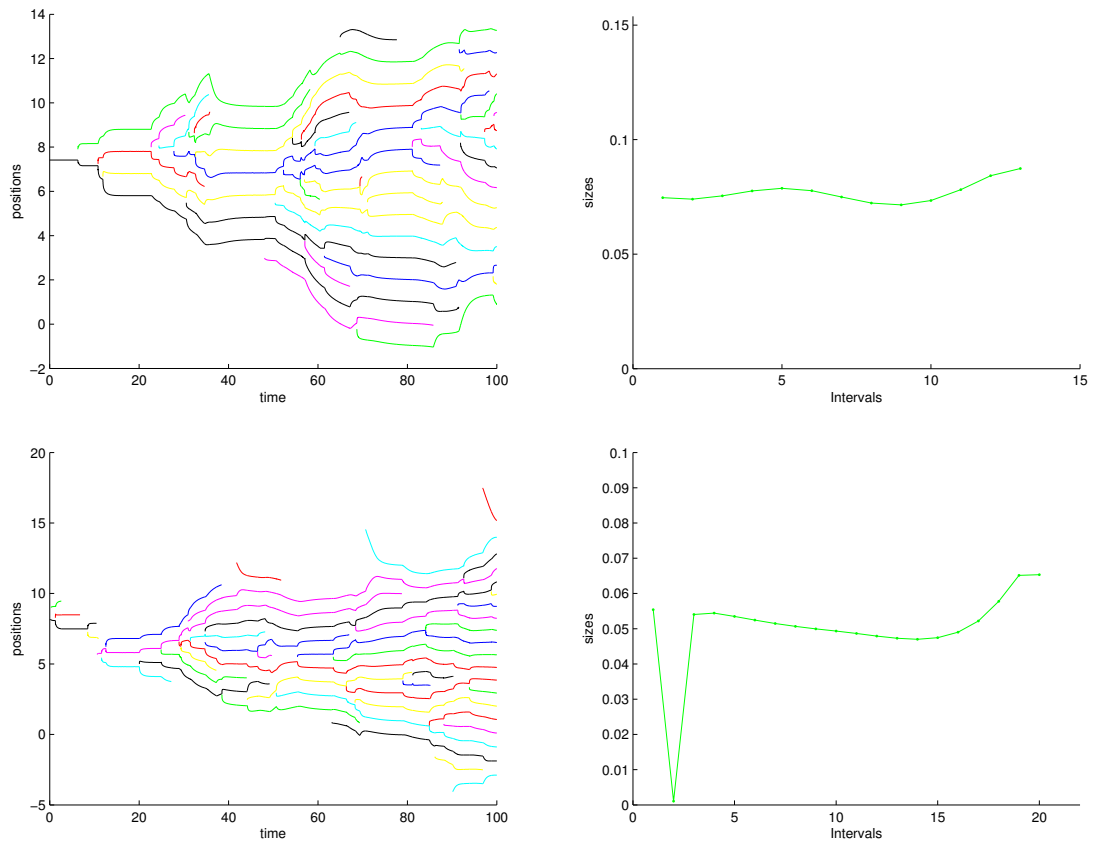


Figure 20: Evolutions in time and final distributions of the spacings for two sample runs of the model of Section 4;  $\xi = 1$ ,  $d = 1$ ,  $m_a = 0$ ,  $m_r = -2$ ,  $\lambda = 0.4$ ,  $\mu = 0.02$ .

## Part II

# Second Project-Birds Take Off

### 1 Introduction

Starlings can form large flocks up to 300,000 birds and yet they manage to organize themselves displaying intense coordinated behavior [23]. Specific interest lies in how a flock begins on the ground and cohesively manages to take flight. These flocks fly more extraordinarily well in a cohesive unit called murmuration. Curiosity lies in how the birds take off into flight as a whole group. Videos have shown that a whole flock can be foraging on the ground, and then take off as a whole. If not all members of the group take off, then the birds that did take off will promptly land again. The flock may choose to try and take off again until all birds in the flock decide to join. Animal collective behavior is observed in many different species such as fish, insects, mammals, and birds. It is an impressive trait in these groups as it shows self organization, or a lack of centralized control. That is, each agent acts only on the limited amount of information that is available to it. However, the agents still manage to act as a unified group [10]. Starlings are a powerful example of how impressive animal collective behavior can be. European Starlings were released in New York City in 1890 and 1891 where sixteen mating pairs survived. Since then their population has expanded rapidly, with the North American population estimated to be around 200 million. As an invasive species, starlings have caused many problems such as an estimated \$800 million in damages to agricultural crops each year. It is important to understand starling flock behavior so that they can be combatted more efficiently [19].

When the flock as a whole takes off, there seems to be an indicator bird that flies

over the flock, signaling the birds to take off. This signal then propagates through the flock until all of the birds end up in flight. Previous studies have determined that starlings are affected by the six to seven birds around them when moving as a flock [7]. Therefore, it seems as though after the indicator bird gives a signal to a specific set of birds on the ground then the remaining birds on the ground take off after each of them see enough of their neighbors.

## 2 Methodology

Videos of starlings leaving the ground were taken using a camcorder from a side view. From the videos several qualitative observations could be made. All of the videos begin with the flock of starlings on the ground. Then, an indicator bird flies in close to the flock and certain birds begin to take off. The indicator bird begins a signal propagation through the flock. If all the birds take off, then they will all fly away together as a whole. If enough of the birds fail to take off into flight, the ones who did take off come back down and land. These observations led to a model simulating the behavior of the flock which was constructed using Matlab software. The contents of this model are described in the model section.

To analyze the videos quantitatively and measure the pixel of the videos, we used ImageJ. ImageJ allowed us to crop the videos so that the birds were all seen but the background was minimized. The videos were then thresholded so that only black and white pixels were recognized. The black pixels in these videos represent the birds or bigger objects, such as trees, and the white pixels represent the background. The video was stacked to images so each time frame was able to be observed. Following that, the black pixels in an image at one time step was subtracted from black pixels in an image at the previous time step. This calculation accounts for the change in number of black pixels as the video progresses. The data of change in pixels was graphed. To obtain the graphs, we processed our video in ImageJ that performs the following:

1. Crops the video to focus on birds part only.
2. Thresholds the video to make it black and white.
3. Crops the video 5 equal pieces from left to right. Figure 22



Figure 21: Orginal video before cropped and substacked

4. For every other part of the video we cropped, uses the grayscale feature,then histogram to list all the counts.
5. Calculates the stardart deviation by copying and pasting all the counts to the Excel file.

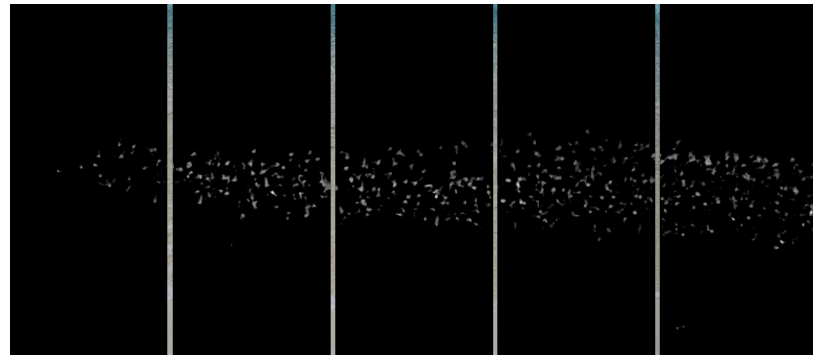


Figure 22: Subtracted and cropped video

It was determined that the change in number of black pixels corresponds to the recruitment of birds in the air. In the model a graph showing number of birds in the air against time was created. Comparing the graph from the observed results in the videos to the results from the model, it was determined that they both follow a similar trend. This insinuates that the model accurately portrays the recruitment of birds. Due to this, we were able to manipulate the varying constants we placed in

the model to find several different results which are believed to describe the actual behavior of flocks.

### 3 Model

Our model uses  $x, y, z$  to represent the position of the bird and  $t$  to represent time.

A constant  $R_{min}$  was introduced as a minimum distance between birds. This ensures that birds will not randomly be placed on top of each other.

The position of each bird is represented by the coordinates  $x_j, y_j, z_j$  with

$$j \in \{1, \dots, N\}$$

To denote the rate of change of position of each bird  $\dot{x}_j, \dot{y}_j, \dot{z}_j$  will be used.

$\dot{x}_j, \dot{y}_j$  will remain 0 for the entire simulation because the main focus is the vertical movement.

The vertical velocity is given by  $\dot{z}_j$ .  $\dot{z}_j$  represents the change in position of the bird based upon  $\varphi$  which will be defined in what follows.  $\delta$  is a time delay and will indicate how fast a bird will react to its signal to take off or not take off.  $c$  is a constant related to the vertical speed.

$$\dot{z}_j(t) = \begin{cases} \varphi_j(t - \delta)c & \text{if } \varphi_j(t - \delta) > 0 \\ 0 & \text{if } \varphi_j(t - \delta) \leq 0, z_j(t) = 0 \\ \varphi_j(t - \delta)c & \text{if } \varphi_j(t - \delta) \leq 0, z_j(t) > 0 \end{cases} \quad (6)$$

This model will use a stimulus variable,  $s_j(t)$ , that will determine which birds take off first. There will be specific birds on the ground that will be stimulated based on their position. These birds will react to an indicator bird, or a stimulus.

$T_s$  is a set time that will represent the amount of time for the activation of the stimulus. The stimulus will only be used for a short amount of time in order to start

the flight of specific birds.

$$s_j(t) = 0 \text{ for any bird if } t > T_s$$

$$s_j(t) = 1 \text{ for stimulated birds if } t < T_s$$

$$s_j(t) = 0 \text{ for non-stimulated birds if } t < T_s$$

Once the stimulated birds have taken off, the birds that are not stimulated will rely on their neighbors to decide whether or not it will take flight.

The variable that will assess whether a bird will take off or will not take off is  $\varphi_j$ :

$$\varphi_j(t) = k_s * s_j(t) + \bar{\varphi}_j(t), \quad (7)$$

where  $k_s$  is a constant representing the birds for the stimulus. The function  $\varphi_j$  is composed of two parts: the stimulus  $s_j$  and  $\bar{\varphi}_j$ , which is defined as

$$\bar{\varphi}_j = \sum_{i \in N_j} \mathbb{1}_{z_i > 0} - k_m, \quad (8)$$

where  $k_m$  is a constant corresponding to the minimum number of neighboring birds necessary for a bird to decide to take off or land.

For the metric model a radius,  $R$ , is used. The area within radius  $R$  will be used by an individual bird to assess the number of birds around it that have taken off or not. If the number of birds that have taken off within the radius is greater than or equal to  $k_m$ , the individual bird will take off. If the number of birds that have taken off within the radius is less than  $k_m$ , the bird will not take off. Hence we define the set of neighbors  $N_j$  as follows:

$$i \in N_j \text{ if } \sqrt{(x_i - x_j)^2 + (y_i - y_j)^2} < R. \quad (9)$$

In the topological model, each bird only considers a certain number,  $N_{topo}$ , of its closest neighbors. To do this we calculated the distance from each bird to every other bird and then isolated the  $N_{topo}$  shortest distances to determine which neighbors each bird would consider.

The Runge-Kutta numerical scheme was used to solve the differential equation (6) and was implemented in Matlab.

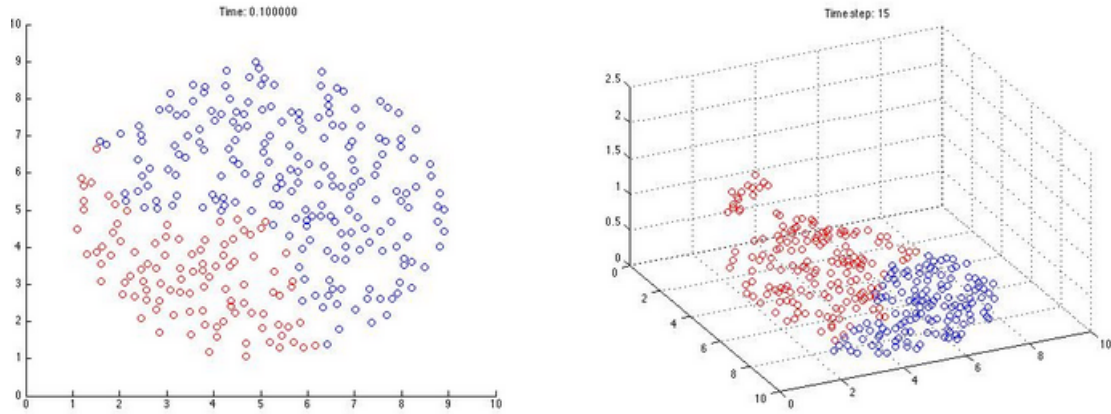


Figure 23: Display from the model.

Figure 23 is a sample of the images that the model creates. On the left is a two-dimensional view of the model and on the right is a three-dimensional view. Red circles indicate birds that have taken off and are in the air while blue circles indicate birds that are on the ground and have not taken off. These images were both created using the topological model. Enough time has passed so all the stimulated birds have taken off as well as a portion of the non-stimulated birds.

## 4 Results

### 4.1 Comparison to Observed Behavior

The data collected from ImageJ when analyzing the videos represents the change in number of black pixels over time. This experimental data correlates to the recruitment of birds in the air over time. Using the model, the number of birds in the air over time was plotted. Figure 25 shows the relationship between the experimental and simulated data. As time increases, the number of birds in the air increases as well and then plateaus at a certain time once the whole flock gets into the air.

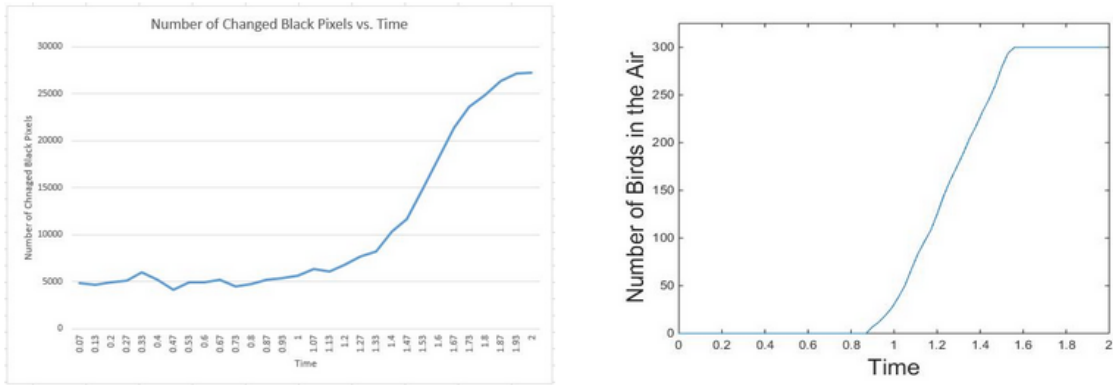


Figure 24: Experimental and simulated data for recruited birds in the air.

The table below indicates the front velocities from the experimental data and the model. The front velocity of the experimental data was calculated using the videos obtained and ImageJ to estimate distances and observe the time. Once the velocity of the experimental data was calculated, the unknown variable for the delay ( $\delta$ ) was adjusted until the velocity of the model was close to the observed velocity. In the topological model all constants were kept the same except for the delay. It was found that  $\delta = 0.1$  seconds. This method for finding the delay was possible for the metric model as well, however there were more unknowns, besides  $\delta$  so it is harder

to accurately match the data. Since the topological model was a better fit, the delay that was found more accurately represents the behavior of the flock.

<b>Flocking Method</b>	<b>Average Velocity of 3 runs (m/s)</b>
Observed Behavior	16.92
Topological	16.22

Figure 25: Experimental and simulated velocities.

## 4.2 Effect of Constants on Front Velocity

The following graphs present the average velocity after ten runs for each data point, at the different sets of parameters listed below. The metric model was used to obtain this data. A linear equation was fit to a graph of distance as a function of time to give the velocity of the signal propagation. All of the tables to the right of the figures express the standard error of the slope for one run at each data point. The results reveal that the error of the linear regression is small. This indicates that the linear regression accurately fits the actual values. These velocities were calculated using arbitrary units and were used to observe behaviors of the model. The velocities only reflect the properties and not the actual velocity.

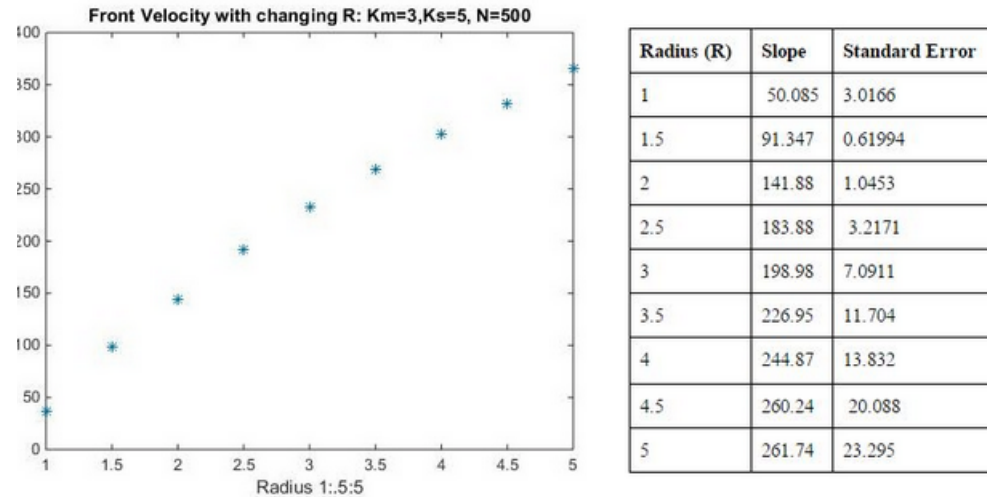


Figure 26: Speed and standard error for changing radius.

Figure 26 represents the change in front velocity as the radius increases from 1 to 5 at intervals of 0.5. As the radius increases the velocity also increases. This is due to the fact that as the radius increases, there is a greater chance of a bird seeing its neighbors in the air.

Figure 27 shows how the front velocity changes as  $N$ , the number of birds in the

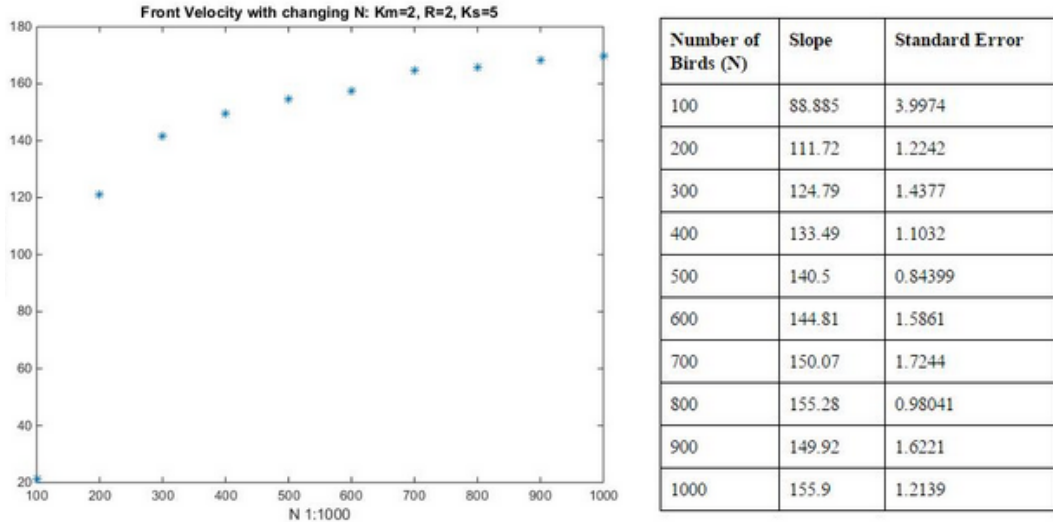


Figure 27: Speed and standard error for changing number of birds.

flock, increases. The front velocity increases as the number of birds increases. However, once the number of birds becomes large enough, the front velocity reaches an equilibrium point and stops increasing.

Figure 28 represents how the front velocity changes as  $k_s$ , the constant in  $\varphi$ , increases.  $k_s$  affects the stimulated birds. This graph shows that as long as  $k_s$  is greater than  $k_m$ , it does not have a noticeable effect on the velocity.

Figure 29 represents how the front velocity changes as  $k_m$  increases. The constant  $k_m$  is in  $\bar{\varphi}$ , which tells the minimum number of neighboring birds necessary for a bird to decide to take off or not take off. This graph shows that the front velocity will be zero, so no birds take off, if  $k_m$  is greater than or equal to  $k_s$ . While  $k_m$  is less than  $k_s$ , the velocity decreases slightly. In Figures 27 and 28 the data points where  $k_s$  is less than  $k_m$ , the birds do not take off therefore the front velocity is zero and no error is computed.

Figure 30 is similar to Figure 28. This graph represents how the front velocity changes as  $k_m$  increases. However, a large  $k_s$  was chosen so that  $k_m$  would never be greater than it. Thus, it is clear that as  $k_m$  increases, as long as it is less than  $k_s$ ,

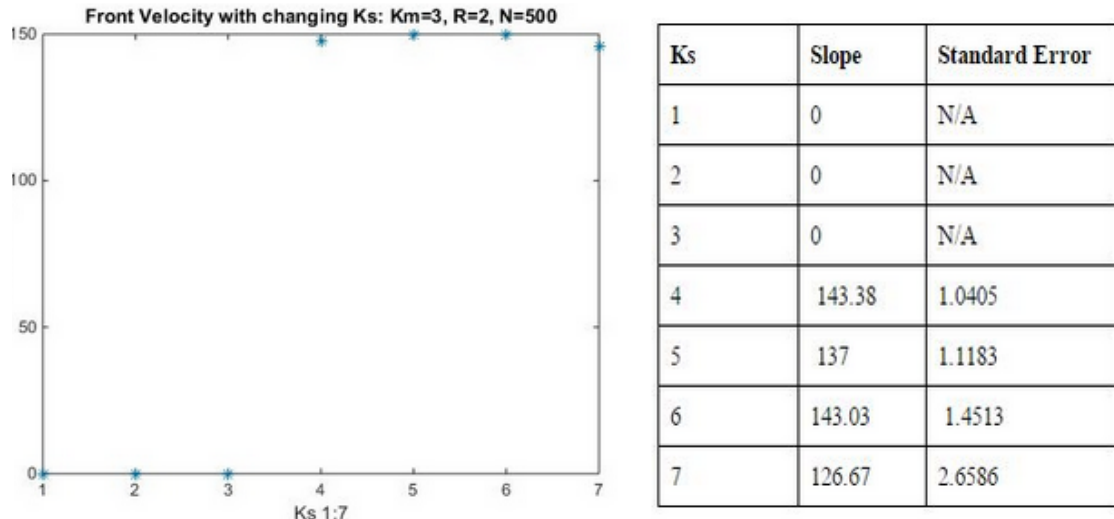


Figure 28: Speed and standard error for changing  $k_s$ .

the front velocity slows.

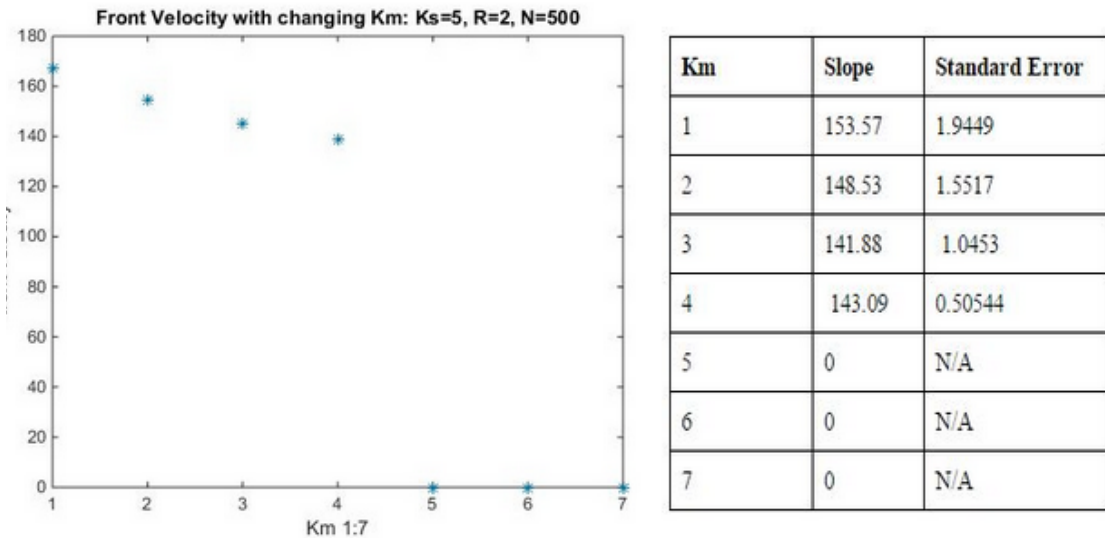


Figure 29: Speed and standard error for changing  $k_m$ .

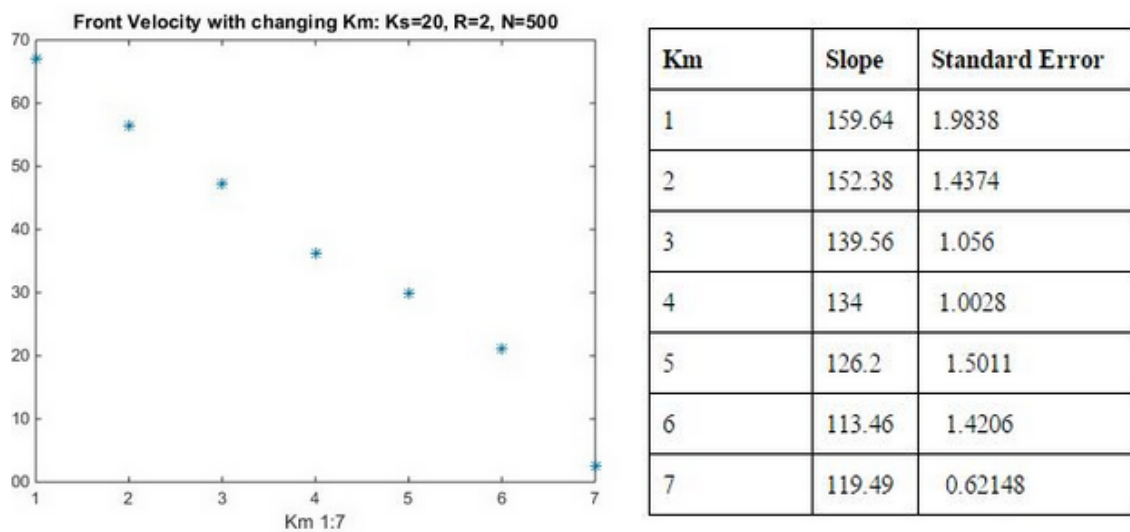


Figure 30: Speed and standard error for changing  $k_m$ .

## 5 Front Length

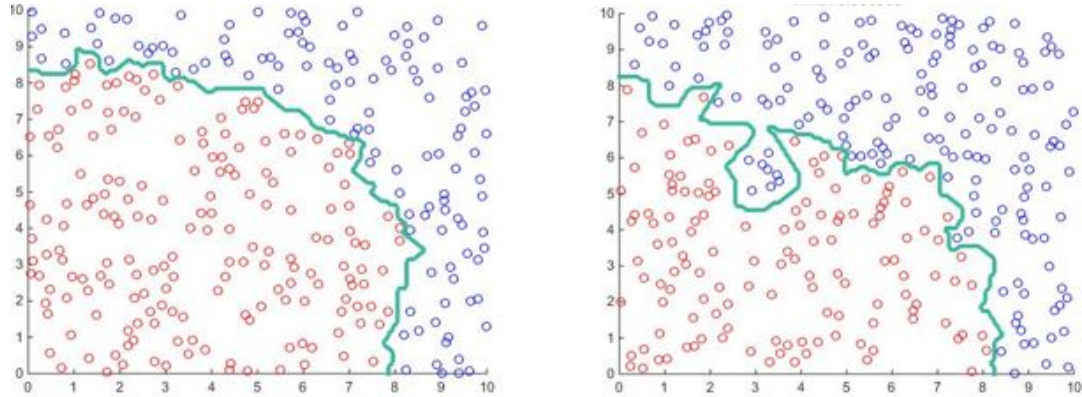


Figure 31: Front line propagating through the flock.

In the model a line that plots around the birds that have just taken off was created. This line progresses through the flock as the signal propagates and the birds take off. It splits the birds that are in the air from the ones that are on the ground. An example of this line is shown in Figure 31. On the left of Figure 31 is the front length shown on the metric model and the left is the front length on the topological model.

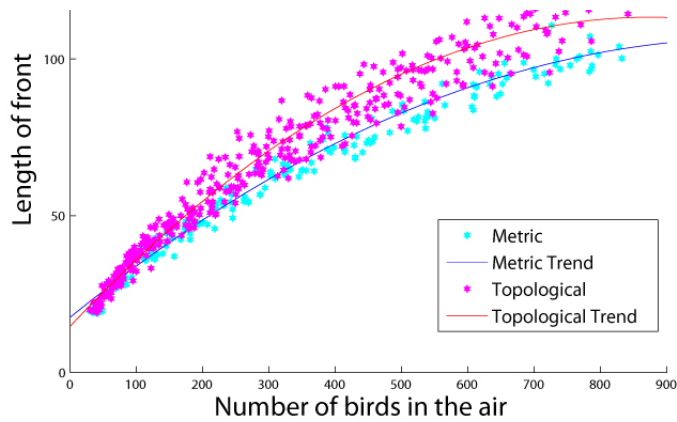


Figure 32: Length of the front vs. number of birds in the air.

The length of this front line was measured for both the metric and topological models. The topological and metric versions were created and a line of best fit was placed to show the average of all the data points.

Figure 32 shows the length of the front compared to the number of birds in the air for metric and topological. Overall, the front length for the topological model is longer than the front length of the metric model. The topological front line can be more irregular which would lead to the longer front line.

## A Appendix: Proof of Proposition 2.1

First we focus on iii). Since  $j \in \mathcal{N}(i)$  implies  $i \in \mathcal{N}(j)$ , then  $\sum_{i=1}^N \dot{x}_i = 0$  and the average of the position sis preserved along solutions.

We now prove i). The right-hand side of (1) is defined and continuous on  $\mathcal{D}$ , thus Peano's Theorem ([13]) ensures existence of a local solution  $x(\cdot)$  in  $\mathbb{R}^N \setminus \mathcal{D}$ . Such solution can be prolonged as long as it does not enter the region  $\mathcal{D}$  or blows up.

Let us define  $d(x(t), \mathcal{D}) = \inf_{x \in \mathcal{D}} \|x - x(t)\|_{\mathbb{R}^n}$  and set:

$$\bar{t} = \inf\{\tau : \limsup_{t \rightarrow \tau^-} \left( \max_i |x_i| + \frac{1}{d(x(t), \mathcal{D})} \right) = +\infty\}$$

We will prove, by contradiction, that  $\bar{t} = +\infty$ , splitting the proof in two steps.

**Step 1.** First we suppose that:

$$\limsup_{t \rightarrow \bar{t}-} \max_i |x_i| = +\infty.$$

Then either  $\limsup_{t \rightarrow \bar{t}-} x_N(t) = +\infty$  or  $\liminf_{t \rightarrow \bar{t}-} x_1(t) = -\infty$ . We deal with the first case, the second being similar by symmetry. We can write:

$$\dot{x}_N = \sum_{j \in \mathcal{N}(N)} |x_j - x_N|^{m_a-1} (x_j - x_N) - \sum_{j \in \mathcal{N}(N)} \xi^{m_a-m_r} |x_j - x_{i_1}|^{m_r-1} (x_j - x_N) \doteq T_1 - T_2. \quad (10)$$

We have  $T_1 \leq 0$ , thus we must have  $\liminf_{t \rightarrow \bar{t}-} T_2 = -\infty$ , which implies

$\liminf_{t \rightarrow \bar{t}-} (x_N(t) - x_{N-1}(t)) = 0$ . Moreover, we deduce  $\limsup_{t \rightarrow \bar{t}-} x_{N-1}(t) = +\infty$ , otherwise from (10) we would get  $\dot{x}_N(t) \leq 0$  when  $x_N(t) > \max x_{N-1}(t) + \xi$ , which contradicts  $\limsup_{t \rightarrow \bar{t}-} x_N(t) = +\infty$ .

Now we can write:

$$\begin{aligned}
\dot{x}_{N-1} &= [|x_N - x_{N-1}|^{m_a-1} - \xi^{m_a-m_r} |x_N - x_{N-1}|^{m_r-1}] (x_N - x_{N-1}) \\
&\quad + \sum_{j \in \mathcal{N}(N-1) \setminus \{N\}} |x_j - x_{N-1}|^{m_a-1} (x_j - x_{N-1}) \\
&\quad - \sum_{j \in \mathcal{N}(N-1) \setminus \{N\}} \xi^{m_a-m_r} |x_j - x_{N-1}|^{m_r-1} (x_j - x_{N-1}) \\
&\doteq T_1 + T_2 - T_3,
\end{aligned}$$

with  $\liminf_{t \rightarrow \bar{t}-} T_1 = -\infty$  and  $T_2 \leq 0$ . Moreover  $T_1$  is bounded from above, which implies  $\liminf_{t \rightarrow \bar{t}-} T_3 = -\infty$  thus  $\liminf_{t \rightarrow \bar{t}-} (x_{N-1}(t) - x_{N-2}(t)) = 0$ . Moreover, we claim that  $\limsup_{t \rightarrow \bar{t}-} x_{N-2}(t) = +\infty$ , otherwise the midpoint  $x_M(t) = \frac{x_N(t) + x_{N+1}}{2}$  would satisfy  $\dot{x}_M(t) \leq 0$  when  $x_N(t) > \sup x_{N-2}(t) + \xi$ , which contradicts  $\limsup_{t \rightarrow \bar{t}-} x_{N-1}(t) = +\infty$ .

We can now reason by recursion and prove that  $\liminf_{t \rightarrow \bar{t}-} (x_N(t) - x_1(t)) = 0$  and  $\limsup_{t \rightarrow \bar{t}-} x_1(t) = +\infty$ , which contradicts iii).

**Step 2.** We proved that

$$\limsup_{t \rightarrow \bar{t}-} \max_i |x_i| < +\infty,$$

then

$$\liminf_{t \rightarrow \bar{t}-} d(x(t), \mathcal{D}) = 0$$

and, by compactness, there exists  $y \in \mathcal{D}$  such that  $\liminf_{t \rightarrow \bar{t}-} \|x(t) - y\|_{\mathbb{R}^N} = 0$ . Let  $i$  be the minimal index such that  $y_i = y_{i+1}$  for some  $y = y(i) \in \mathcal{D}$  satisfying

$\liminf_{t \rightarrow \bar{t}-} \|x(t) - y(i)\|_{\mathbb{R}^N} = 0$ . Then we can write:

$$\begin{aligned}\dot{x}_i &= \sum_{j \in \mathcal{N}(i), j < i} [|x_j - x_i|^{m_a-1} - \xi^{m_a-m_r} |x_j - x_i|^{m_r-1}] (x_j - x_i) \\ &\quad + \sum_{j \in \mathcal{N}(i), j > i} |x_j - x_i|^{m_a-1} (x_j - x_i) \\ &\quad - \sum_{j \in \mathcal{N}(i), j > i} \xi^{m_a-m_r} |x_j - x_i|^{m_r-1} (x_j - x_i) \\ &\doteq T_1 + T_2 - T_3.\end{aligned}$$

By definition of  $i$  we have that  $\liminf_{t \rightarrow \bar{t}-} (x_i(t) - x_{i-1}(t)) > 0$ , thus  $T_1$  remains bounded. Moreover  $T_2$  is bounded by definition and  $T_3 \geq 0$ . This gives that

$\limsup_{t \rightarrow \bar{t}-} \dot{x}_i(t)$  is bounded, thus there exists the limit of  $x_i(t)$  for  $t \rightarrow \bar{t}-$  and  $\lim_{t \rightarrow \bar{t}-} x_i(t) = y(i)_i$ . Now consider the index  $i+1$  and assume

$l = \limsup_{t \rightarrow \bar{t}-} x_{i+1}(t) > y(i)_{i+1}$ . For  $\delta$  sufficiently small,  $x_i(t) < y(i)_i + \frac{1}{3}(l - y(i)_i)$  for  $t \geq \bar{t} - \delta$ . But then  $\dot{x}_{i+1}(t)$  is uniformly bounded above whenever

$x_{i+1}(t) > y(i)_{i+1} + \frac{2}{3}(l - y(i)_i)$  and  $t \geq \bar{t} - \delta$ , which contradicts the definition of  $l$  and the fact that  $y(i)_{i+1} = y(i)_i$ . Thus we deduce  $\lim_{t \rightarrow \bar{t}-} x_{i+1}(t) = y(i)_{i+1}$ . More generally, for every index  $\ell > i$  such that  $\liminf_{t \rightarrow \bar{t}-} x_\ell(t) = y(i)_i$  we get that

$\lim_{t \rightarrow \bar{t}-} x_\ell(t) = y(i)_i$ . Now, let  $k > i$  be the greatest index such that

$\liminf_{t \rightarrow \bar{t}-} x_k(t) = y(i)_i$  (and thus  $\lim_{t \rightarrow \bar{t}-} x_k(t) = y(i)_i$ ). Then we have that either  $k = N$  or  $\liminf_{t \rightarrow \bar{t}-} (x_{k+1}(t) - x_k(t)) > 0$ . In both cases we can write:

$$\begin{aligned}\dot{x}_k &= \sum_{j \in \mathcal{N}(k), j > k} [|x_j - x_k|^{m_a-1} - \xi^{m_a-m_r} |x_j - x_k|^{m_r-1}] (x_j - x_k) \\ &\quad + \sum_{j \in \mathcal{N}(k), j < k} |x_j - x_k|^{m_a-1} (x_j - x_k) \\ &\quad - \sum_{j \in \mathcal{N}(k), j < k} \xi^{m_a-m_r} |x_j - x_k|^{m_r-1} (x_j - x_k) \\ &\doteq T_1 + T_2 - T_3.\end{aligned}$$

From  $\liminf_{t \rightarrow \bar{t}-} (x_{k+1}(t) - x_k(t)) > 0$  (or  $k = N$ ) we deduce that  $T_1$  is bounded, while  $T_2$  is bounded by definition and  $T_3 < 0$ . Since  $\lim_{t \rightarrow \bar{t}-} x_k(t) = y(i)_i$  we deduce  $\lim_{t \rightarrow \bar{t}-} \dot{x}_k(t) = +\infty$  which gives a contradiction.

We just proved i) and the fact that  $\bar{t} = +\infty$  implies also ii).

## References

- [1] I. Aoki. An analysis of the schooling behavior of fish: internal organization and communication process. *Bull. Ocean Res. Inst. Univ. Tokyo*, 12:1–65, 1980.
- [2] M. Ballerini, N. Cabibbo, R. Candelier, A. Cavagna, E. Cisbani, I. Giardina, V. Lecomte, A. Orlandi, G. Parisi, A. Procaccini, M. Viale, and V. Zdravkovic. Interaction ruling animal collective behavior depends on topological rather than metric distance: Evidence from a field study. *105(4):1232–1237*, 2008.
- [3] M. Ballerini, N. Cabibbo, R. Candelier, A. Cavagna, E. Cisbani, I. Giardina, A. Orlandi, G. Parisi, A. Procaccini, M. Viale, and V. Zdravkovic. Empirical investigation of starling flocks: a benchmark study in collective animal behaviour. *76:201–215*, July 2008.
- [4] N. Bellomo and J. Soler. On the mathematical theory of the dynamics of swarms viewed as complex systems. *Mathematical Models and Methods in Applied Sciences*, 22:1140006, 2012.
- [5] I. D. Couzin, J. Krause, N. R. Franks, and S. A. Levin. Effective leadership and decision-making in animal groups on the move. *433(7025):513–516*, 2005.
- [6] I. D. Couzin, J. Krause, R. James, G. D. Ruxton, and N. R. Franks. Collective memory and spatial sorting in animal groups. *218:1–11*, 2002.
- [7] E. Cristiani, P. Frasca, and B. Piccoli. Effects of anisotropic interactions on the structure of animal groups. *62(4):569–588*, 2011.
- [8] F. Cucker and J.-G. Dong. A conditional, collision-avoiding, model for swarming. *Discrete and Continuous Dynamical Systems*, 34(3):1009–1020, 2014.
- [9] F. Cucker and S. Smale. Emergent behavior in flocks. *52(5):852–862*, 2007.
- [10] I. Giardina. Collective behavior in animal groups: theoretical models and empirical studies. *HFSR Journal*, 2(4):205–219, 2008.
- [11] G. R. Grimmett and D. R. Stirzaker. *Probability and random processes*. Oxford university press, 2001.
- [12] S. Gueron, S. A. Levin, and D. I. Rubenstein. The dynamics of herds: from individuals to aggregations. *182:85–98*, 1996.
- [13] J. Hale. *Ordinary Differential Equations*. Krieger Publishing, Huntington, NY, 1980.
- [14] W. D. Hamilton. Geometry for the selfish herd. *31:295–311*, 1971.
- [15] A. Huth and C. Wissel. The simulation of the movement of fish schools. *156(3):365–385*, 1992.

- [16] Y. Inada and K. Kawachi. Order and flexibility in the motion of fish schools. *214(3):371–387*, 2002.
- [17] J. Krause and G. D. Ruxton. *Living in groups*. Oxford Series in Ecology and Evolution. Oxford, 2002.
- [18] H. Kunz and C. K. Hemelrijk. Artificial fish schools: collective effects of school size, body size, and body form. *Artificial Life*, 9(3):237–253, 2003.
- [19] G.M. Linz, H.J. Homan, S.M. Gaulker, L.B. Penry, and W.J. Bleir. European starlings: a review of an invasive species with far-reaching impacts. managing vertebrate invasive species: proceedings of an international symposium. *USDA/APHIS Wildlife Services, National Wildlife Research Center, Fort Collins, Colorado, USA*, page 24.
- [20] R. Lukeman, Y.-X. Li, and L. Edelstein-Keshet. A conceptual model for milling formations in biological aggregates. *Bulletin of Mathematical Biology*, 71(2):352–382, 2009.
- [21] A. Mogilner, L. Edelstein-Keshet, L. Bent, and A. Spiros. Mutual interactions, potentials, and individual distance in a social aggregation. *47(4):353–389*, 2003.
- [22] J. K. Parrish, S. V. Viscido, and D. Grunbaum. Self-organized fish schools: An examination of emergent properties. *Biological Bulletin*, 202(3):296–305, 2002.
- [23] D.J. Pearce, A. M. Miller, G. Rowlands, and M.S. Turner. Role of prejection in the control of birds flocks. *Proceedings of the National Academy of Sciences*, page 29, 2014.
- [24] D. J. T. Sumpter. The principles of collective animal behaviour. *Phil. Trans. R. Soc. B*, 361:5–22, 2006.
- [25] T. Vicsek, A. Czirók, E. Ben-Jacob, I. Cohen, and O. Shochet. Novel type of phase transition in a system of self-driven particles. *75(6):1226–1229*, 1995.
- [26] K. Warburton and J. Lazarus. Tendency-distance models of social cohesion in animal groups. *150:473–488*, 1991.

**MATLAB SCRIPT****1) Simulation wire.m**

```
N=12; % # birds
Tmax=50; % final time for simulation
Nrun=30; % # random instances
xi=[1/3 1/2 1 2 3];
d=[1 2 3 4 5];
der=0.1;
colors='ymcrgbk';
% parameters of interaction law are in 'interactionRHS'
% running simulation
allDist=zeros(N-1,Nrun);
for j=1:length(xi)
    for i=1:length(d)
        sum_length=0;
        tfs=0;
        clear gra t;
        for r=1:Nrun

            x0=10*rand(N,1);
            x0=sort(x0);
            x0=[x0;d(i);xi(j)];
            [t,x]=ode45(@interactionRHS,[0,Tmax],x0);
            x=x(:,1:N);
            if sum(sum(isnan(x)))~=0 && r>1
                r=r-1;
            else
                for k=1:N
                    gra(:,k)=gradient(x(:,k),t);
                end
                if r<Nrun
                    clear t gra;
                end
                [m,discard]=size(x);
                xfinal=x(m,:);
                xfinal=sort(xfinal);
                dist=zeros(N-1,1);
                for h=1:N-1
                    dist(h)=-xfinal(h)+xfinal(h+1);
                end
                total_length=xfinal(N)-xfinal(1);
                allDist(:,r)=dist/total_length;
                sum_length=sum_length+total_length;
            end
        end
        ave_length{j}(i,1)=sum_length/Nrun;
        ave_length{j}(i,2)=xi(j)*(N-1)/sqrt(d(i));

        meanDist=mean(allDist,2);
        figure(j+length(xi))
        hold on
        plot(meanDist, colors(i), 'marker', '.')
        data(:,i+(j-1)*length(d))=meanDist;
        legendStr{i}=['d=' num2str(d(i))];
    end
end
```

```

axis([0 N+1 0 2/(N-1)])

figure(j+2*length(xi))
loglog(ave_length{j}, '.-')

end

figure(j)
plot(t, gra)
xlabel('Time')
ylabel('Derivative')

figure(j+length(xi))
xlabel('Intervals')
ylabel('Sizes')
legend(legendStr, 'location', 'best');
titleStr=['$\xi=' num2str(xi(j)) ' N=' num2str(N), '$'];
title(titleStr, 'interpreter', 'latex')
hold off

figure(j+2*length(xi))
xlabel('d')
ylabel('length')
legend('Simulated', 'Theoretical')
title(titleStr, 'interpreter', 'latex')
axis([0 10 0 100])
hold off

figure(j+3*length(xi))
plot(t,x)
xlabel('Time')
ylabel('Positions')

```

end

## 2) Interaction RHS Function

```

function [xdot]=interactionRHS(t,x)
% [xdot]=interactionRHS(t,x)
% Editing the function one can set the parameters of the interaction
law

% parameters of the interaction law
% xi=1; % desired distance
% d=20;
m=-1; % attraction power law (nonnegative) (usually it is 0 or 1)
n=-2; % repulsion power law (negative!) (usually it is -1)

% writing interaction matrix
xi=x(end);
d=x(end-1);
x=x(1:end-2);
N=length(x);
A=zeros(N,N);
for h=1:N

```

```

for k=1:N
    if h~ =k && abs(h-k) <=d
        A(h,k)=1;
    end
end
x=sort(x);

%%% computing rhs, keeping the right sign

X=ones(N,1)*x'-x*ones(1,N);

attrComp=X.^ (m+1);
if mod(m,2)==1
    attrComp=attrComp.*sign(X);
end
if m<0
    for h=1:N, attrComp(h,h)=0; end
end

repComp=X.^ (n+1);
if mod(n,2)==1
    repComp=repComp.*sign(X);
end
if n<0
    for h=1:N, repComp(h,h)=0; end
end

xdot=[sum(A.*attrComp-xi^(m-n)*A.*repComp,2)/(2*d);0;0];

```

### 3) Birds Taking-Off 2D and 3D

```

T=1; %end of time
Dview = 3; % Choice of display (2 for 2D, 3 for 3D)
scheme = 'RK'; % 'EU' for Euler, 'RK' for Runge-Kutta
eps = 0;%10^(-5);
dt = 0.01; % time-step
t = 0:dt:T; % time vector
Nt = length(t); % Number of time-steps

global R;
R=1.5; %radius

global Ks;
Ks=5; %constant for the stimulus

global Km;
Km=3; %constant in phibar

global Ts;
Ts=.1; %threshold time

global c;

```

```

c=1; %constant in zdot

global N;
N=500; %total number of birds

% Initial conditions
z0=zeros(N,1);
x0=10*rand(N,1);
y0=10*rand(N,1);
X0=[x0;y0;z0];

% Matrix of positions at each time
X = zeros(Nt,3*N);
X(1,:) = X0;

switch scheme
    case 'RK'
        for it = 1:Nt-1
            k1 = dyn(t(it), X(it,:));
            k2 = dyn(t(it)+dt/2, X(it,:)+dt/2*k1);
            k3 = dyn(t(it)+dt/2, X(it,:)+dt/2*k2);
            k4 = dyn(t(it)+dt, X(it,:)+dt*k3);
            X(it+1,:) = X(it,:) + dt/6*(k1 + 2*k2 + 2*k3 + k4);
        end

    case 'EU'
        for it = 1:Nt-1
            dX = dyn(t(it),X(it,:));
            X(it+1,:) = X(it,:) + dX *dt;
        end
    end

if Dview == 3
    for i=1:length(t);
        x=X(i,1:N);
        y=X(i,N+1:2*N);
        z=X(i,2*N+1:3*N);
        color2 = zeros(N,3);
        for j = 1:N
            if z(j)>eps
                color2(j,:)=[1 0 0];
            else
                color2(j,:)=[0 0 1];
            end
        end
        scatter3(x,y,z,[], color2)
        %view([0 0])
        view([64.5 38])
        axis([0 10 0 10 0 10])
        str=sprintf('Time:%f',t(i));
        str=sprintf('Time step: %d',i);
        title(str)
        pause(1)
    end
end

```

```

end

if Dview == 2
    for i=1:length(t);
        x=X(i,1:N);
        y=X(i,N+1:2*N);
        z=X(i,2*N+1:3*N);
        color2 = zeros(N,3);
        for j = 1:N
            if z(j)>0
                color2(j,:)=[1 0 0];
            else
                color2(j,:)=[0 0 1];
            end
        end
        scatter(x',y',[ ],color2)
        str=sprintf('Time: %f',t(i));
        title(str)
        axis([0 10 0 10])
        pause(.75)
    end
end

```

#### 4) Dynamics Function

```

function [ dX ] = dyn( t,X )
%   DYNAMICS function
%   gives dX which is concatenated vector of
%   zeros for xdot, ydot and values of zdot
global N;
global c;

eps = 10^(-5);

dy=zeros(N,1);
dx=zeros(N,1);
dz=zeros(N,1);
phi=ComputePhi(t,X);
z=X(2*N+1:3*N);

for i=1:N
    if phi(i)>eps
        dz(i)=c*phi(i);
    end
    if phi(i)<=eps
        if z(i)>eps
            dz(i)=-c*abs(phi(i));
        end
        if (abs(z(i))<=eps) || (z(i)<-eps)
            dz(i)=0;
        end
    end
end
dX=[dx;dy;dz]';

```

```
end
```

## 5) Compute PhiBar

```
function [ PhiBar ] = ComputePhiBar(X)
% Compute PhiBar
%   Number of birds it sees in flight
global N;
global Km;
global R;
IndSum=zeros(N,1);
x=X(1:N);
y=X(N+1:2*N);
z=X(2*N+1:3*N);

for i=1:N
    for j=1:N
        if (sqrt(((x(j)-x(i))^2)+((y(j)-y(i))^2))<R) && (z(j)>0)
            IndSum(i)=IndSum(i)+1;
        end
    end
end

VKm=Km*ones(N,1);

PhiBar=IndSum-VKm;
end
```

## 6) PhiBar Function

```
function [ output_args ] = PhiBar( input_args )
%UNTITLED6 Summary of this function goes here
%   Detailed explanation goes here

end
```